Carbohydrate Polymers 90 (2012) 1120–1126

Contents lists available at SciVerse ScienceDirect

Carbohydrate Polymers

journal homepage: www.elsevier.com/locate/carbpol

Synthesis and thermal characterization of xylan-*graft*-polyacrylonitrile

Cüneyt H. Ünlü, N. Simge Öztekin, Oya Galioğlu Atıcı*

Istanbul Technical University, Faculty of Science and Letters, Department of Chemistry, Maslak TR34469, Istanbul, Turkey

ARTICLE INFO

Article history:
Received 23 November 2011
Received in revised form 3 June 2012
Accepted 18 June 2012
Available online 25 June 2012

Keywords:
Xylan
Polyacrylonitrile
Ceric ammonium nitrate
Thermal characterization
Graft copolymer

ABSTRACT

In this study emulsion polymerization of acrylonitrile using xylan from agricultural waste material (corn cob) and cerium ammonium nitrate was investigated in terms of catalyst acid. Stock ceric solutions were prepared using either nitric or perchloric acid as catalyst. Optimum conditions were determined using different parameters such as reaction time, temperature, and component concentrations. Nitric acid catalyzed reactions resulted in maximum conversion ratio (96%) at 50 °C, 1 h where ceric ion, acrylonitrile, xylan, and catalyst concentrations were 21.7 mmol l^{-1}, 0.5 mol l^{-1}, 0.2% (w/v), and 0.1 mol l^{-1}, respectively. However, 83% conversion was obtained with perchloric acid catalysis at 27 °C, 1 h where concentrations were 5.4 mmol l^{-1}, 0.8 mol l^{-1}, 0.5% (w/v), and 0.2 mol l^{-1}, respectively. Copolymer synthesis using perchloric acid was realized at milder conditions than using nitric acid. Thermal analyses of obtained polymers were conducted to characterize copolymers. Results showed that calculated activation energy, maximum degradation temperature, and heat of thermal decomposition changed relying mainly on molecular weight.

1. Introduction

Xylan, which is a naturally occurring polysaccharide, is composed of neutral sugars (mainly xylose and arabinose) and small portions of uronic acid (glucuronic acid and 4-*O*-methyl derivative). It can be extracted from wastes of annual crops (e.g. corn cobs and wheat straw) under oxidizing alkaline conditions (Doner & Hicks, 1997; Ebringerová, Hromádková, Alföldi, & Hribalová, 1998; Sun, Tomkinson, Geng, & Wang, 2000; Xiao, Sun, & Sun, 2001). More than 25% corn cobs' dry weight consist of xylan, and this occurrence makes the corn cobs one of the the main resources. Xylan can find application in fields including thickener (Doner & Hicks, 1997), additive to plastics (due to increasing their stretch, breaking resistance, and makes them more susceptible to biodegradation) (Gáspár, Juhász, Szengyel, & Réczey, 2005). Ceric ions are versatile reagents which are used for oxidations of many organic functional groups (Nagarajan & Srinivasan, 1998; Pottenger & Johnson, 1970) and they can be used as redox initiators in aqueous solutions for copolymerization of vinyl monomers such as acrylonitrile and acrylamide (Atici, Akar, Ayar, & Mecit, 1999; Lutfor, Sidik, Haron, Rahman, & Ahmad, 2003; Mino & Kaizerman, 1958). Properties of the products are involved with the type of the reducing agent, temperature, catalyst type and concentration (Czappa, 1974). Radicals are produced from reducing agents (i.e. alcohol, polyol, ketone, aldehyde, amine, carboxylic acid, hydroxy acid, or amino acid) in several steps. Offered mechanisms show that a complex forms between reducing agent and Ce^{4+}, then this complex decomposes giving a free radical and Ce^{3+} in acidic medium. Formed radicals attack vinyl monomers to start a polymerization, if there are any, in reaction medium. Polysaccharides can also be employed as reducing agent for graft copolymerization (Galioğlu, Soydan, Akar, & Saraç, 1994; Khullar, 2008; Mishra, Clark, Vij, & Daswal, 2008; Pourjavadi & Zohuriaan-Mehr, 2002b); however, ceric ions can also lead to oxidation (Pottenger & Johnson, 1970). Equilibrium between oxidation and polymerization can be controlled via reaction conditions. Studies about polymerizations involved with xylan and ceric ion were mainly on the effect of component concentrations, oxygen presence, etc. (Mishra et al., 2008; Pourjavadi & Zohuriaan-Mehr, 2002a, 2002b); none of them was about the role of catalyst type on polymerization conditions.

This work mainly focuses on the effect of acid catalyst and thermal characterization of polyacrylonitrile copolymers. Effect of acid catalysts on redox polymerization was studied; initiator and reducing agent were ceric ammonium nitrate and xylan. Nitric acid (HNO_3) and perchloric acid ($HClO_4$) were used as catalysts in initiator solution. Optimum conditions for obtaining xylan-*graft*-polyacrylonitrile copolymers (X–PAN) were searched for maximum conversion. Obtained copolymers were characterized using viscometric, spectral, and thermal methods. Thermal characterizations of obtained copolymers were also done in terms of activation energy of decomposition and heat of decomposition.

---

* Corresponding author. Tel.: +90 212 285 3228; fax: +90 212 285 6386.
E-mail address: atici@itu.edu.tr (O.G. Atıcı).

0144-8617/$ – see front matter © 2012 Elsevier Ltd. All rights reserved.
http://dx.doi.org/10.1016/j.carbpol.2012.06.053

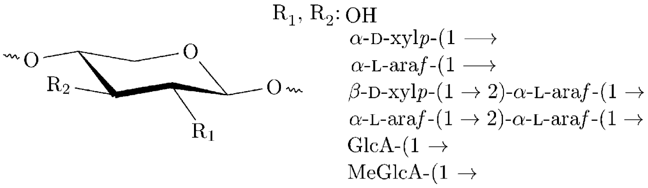

Scheme 1. Simplified representation of xylan.

2. Experimental

2.1. Materials and methods

Corn cobs were collected locally from Adapazarı, Turkey, and xylan was extracted from these corn cobs via alkaline peroxide treatment using procedure described elsewhere (Ünlü, Günister, & Atıcı, 2009). Acrylonitrile monomer, ceric ammonium nitrate (CAN), nitric acid (65%, 1.40 g ml^{-1}), and perchloric acid (70%, 1.67 g ml^{-1}) were Merck brand, and were used as received.

FTIR spectra were recorded on Thermo Nicolet 380 in 4000–400 cm^{-1} region, using KBr pellets with 1% (w/w) sample concentration.

Molecular weight measurements of X–PAN copolymers were done using capillary viscometry. Relative viscosity of the samples was measured using Ubbelohde Typ I viscometer, and sequential dilutions were performed for different concentrations. Intrinsic viscosity values were calculated via Solomon–Ciuťa equation for each point (Pamies, Cifre, del Carmen López Martínez, & de la Torre, 2008; Solomon & Ciuťa, 1962), where $[\eta]$, η_{sp}, η_{rel}, and C were intrinsic viscosity (dl g^{-1}), specific viscosity, relative viscosity, and concentration (g dl^{-1}).

$$[\eta] = \frac{\sqrt{2 \cdot (\eta_{sp} - \ln \eta_{rel})}}{C}$$

Molecular weight (M_V) determination of obtained copolymers was done using intrinsic viscosity and Mark–Houwink equation for polyacrylonitrile ($[\eta] = 3.35 \times 10^{-4} M_V^{0.72}$) in DMF at 30 °C (Shibukawa, Sone, Uchida, & Iwahori, 1968).

Differential scanning calorimetry (DSC) measurements were performed under N_2 atmosphere on TA Instruments Q10 model DSC. Samples were first heated to 130 °C to evaporate adsorbed water, then cooled to −50 °C and reheated to 400 °C; heating (cooling) rate was 10 °C min^{-1}. Heat of decomposition was calculated using area under curve from plot of heatflow (W g^{-1}) versus time (s). Thermogravimetric analyses (TGA) were done with TA Instruments Q50 heating samples from ambient temperature to 700 °C with a rate of 10 °C min^{-1}. Activation energy of decomposition was calculated using TGA data following Broido's method (Broido, 1969). Calculations were carried out using Python 2.7 with NumPy and SciPy modules.

2.2. Polymerization of acrylonitrile

Xylan was dissolved in water and solution was stirred at reaction temperature for 30 min. Then acrylonitrile was added to the solution and stirred for an additional 15 min. Polymerization was initiated with dropwise addition of stock ceric solution in 10 min. After 1-h polymerization, reaction was stopped by pouring the mixture into 500 ml water. Obtained copolymer was washed first with

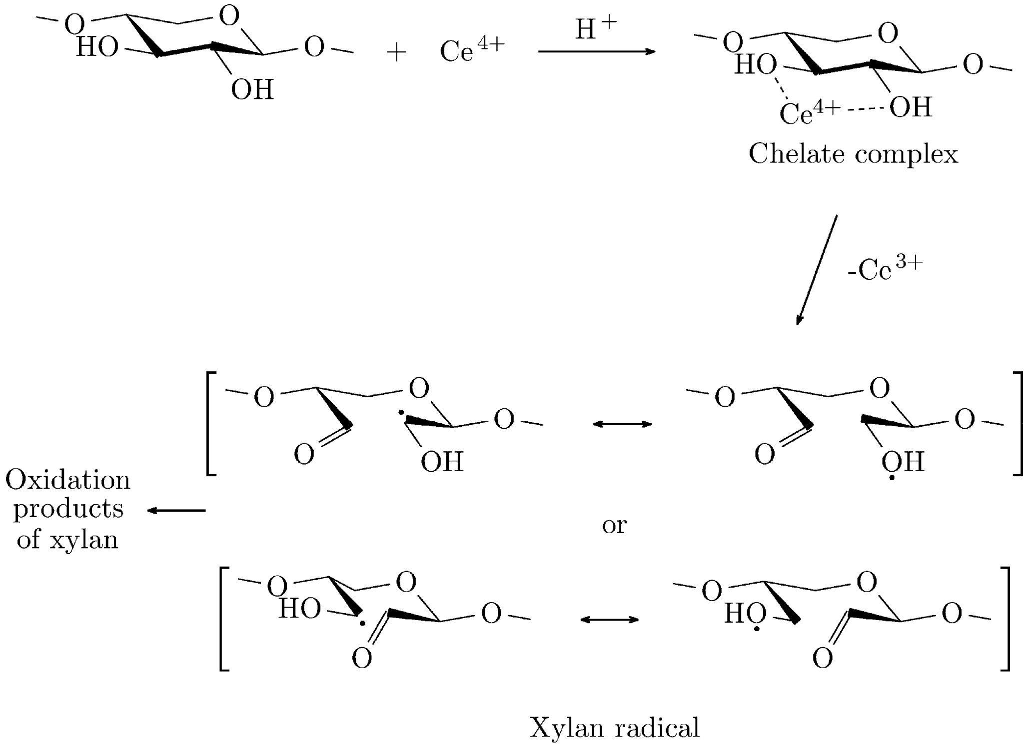

Scheme 2. Reaction mechanism of oxidation of carbohydrates with ceric ion.

$$\underline{\text{Radical generation}}$$

$$Xylan - H + Ce^{4+} \xrightarrow{k} [Complex] \xrightarrow{k_d} X\dot{y}lan + Ce^{3+} + H^+$$

$$\underline{\text{Chain initiation}}$$

$$X\dot{y}lan + M \xrightarrow{k_1} Xylan - \dot{M}$$

$$M + Ce^{4+} \xrightarrow{k_2} \dot{M} + Ce^{3+} + H^+$$

$$\underline{\text{Propagation}}$$

$$Xylan - \dot{M} + nM \xrightarrow{k_{p1}} Xylan - \dot{M}_{n+1}$$

$$\dot{M} + mM \xrightarrow{k_{p2}} \dot{M}_{m+1}$$

$$\underline{\text{Termination}}$$

$$Xylan - \dot{M}_{n+1} + Xylan - \dot{M}_{n+1} \xrightarrow{k_{t1}} Graft\ copolymer$$

$$Xylan - \dot{M}_{n+1} + \dot{M}_{m+1} \xrightarrow{k_{t2}} Graft\ copolymer$$

$$\dot{M} + \dot{M}_{m+1} \xrightarrow{k_{t3}} Homopolymer$$

$$X\dot{y}lan + Ce^{4+} \xrightarrow{k_{ox1}} Oxidation\ products + Ce^{3+} + H^+$$

$$Xylan - \dot{M}_{n+1} + Ce^{4+} \xrightarrow{k_{ox2}} Xylan - M_{n+1} + Ce^{3+} + H^+\ \text{(Oxidation)}$$

Scheme 3. Polymerization reaction initiated with ceric ion.

acetone, then with hot water. X–PAN were dried in air, then in vacuum and analyses for characterizations were carried out.

Blank experiments were carried out using the same procedure; however, xylan was not used for polymerization initiation.

3. Results and discussion

Xylan is a heteropolysaccharide composed of β-D-xylopyranose (xyl*p*), α-L-arabinofuranose (ara*f*), α-D-glucuronic acid (GlcA), and 4-*O*-methyl-α-D-glucuronic acid (MeGlcA) (Scheme 1). Main chain is formed by anhydroxylopyranose units having 1 → 4 connections and has side chains, which are composed of glucuronic acid, mono- and disaccharide residues at 2 and 3 position. Xylan, having many hydroxyl sites like cellulose and starch, is expected to give reactions of other polysaccharides, including oxidation with ceric ions. When carbohydrates and ceric ion react a chelate-complex is formed between oxygen atoms and cerium (Scheme 2). Then the complex decomposes giving a radical on either carbon or oxygen atoms and this radical may further react with ceric ions to give oxidation products and cerous ion. Ceric ion and monomer can also react giving a monomer-radical, which can lead to homopolymerization. Formation of the monomer-radical can be controlled via reaction conditions. The radicalic species can start polymerization reactions if there are vinyl monomers in reaction medium (Scheme 3). Blank, using no reducing agent, experiments are performed in order to determine and eliminate the formation conditions of the homopolymer chains. Then copolymerization conditions are adjusted to give trace amounts (preferably none) of homopolymer. No polymerization occurred during blank experiments indicating xylan was needed for radical generation.

3.1. *Polymerization of acrylonitrile*

3.1.1. *Grafting acrylonitrile onto xylan using CAN in HNO_3*

Optimum condition was searched changing concentrations of the reagents, properties of stock solution (HNO_3 and CAN concentrations), and reaction temperature (Table 1). Varying reaction temperature caused a peak in conversion (77%) about 50 °C, higher (70 °C) and lower (35 °C) temperatures resulted in decrease conversion (57 and 22%); M_V of the copolymers was also affected from conversion, higher the value of the conversion higher the M_V (102, 139, and 8 kDa for conversion ratios of 57, 77, and 22%). Lowering HNO_3 concentration from 0.5 to 0.1 affected conversion negatively (decreased to 64 from 77%); it also resulted in a fall in M_V from 139 to 62 kDa. But higher CAN concentration resulted in the best conversion percentage with 0.1 mol l^{-1} HNO_3. Both conversion ratio and M_V were the highest (96%, 249 kDa) as CAN concentration was 21.7 mmol l^{-1}. Conversion ratio was weakly affected from concentration of xylan or monomer under these circumstances. When xylan concentration was changed from 0.2 to 0.5% conversion remained fairly same; however, M_V of obtained copolymer almost doubled (139–242 kDa). This occurrence could be attributed to increase reducing agent concentration leading to multiple possible radical sites (the more the reducing agent, the more the radical sites).

Optimum condition was found as 21.7 mmol l^{-1} CAN in 0.1 mol l^{-1} nitric acid gave maximum conversion (96%) at 50 °C using 0.2% (w/v) xylan and 0.49 mol l^{-1} acrylonitrile for 1-h reaction; copolymer species obtained under these conditions were labeled as X–PAN$_{HNO_3}$.

3.1.2. *Grafting acrylonitrile onto xylan using CAN in $HClO_4$*

Optimum condition was also searched for $HClO_4$ catalyzed polymerization reactions. In order to prevent oxidation, ambient temperature was used as oxidation potential of $HClO_4$ was higher than HNO_3 (Czappa, 1974). Acid concentration was determined as 0.2 mol l^{-1} for polymerization. Low CAN concentrations (5.5 mmol l^{-1}) were enough to start polymerization efficiently, however, higher CAN concentration (10.9 mmol l^{-1}) caused the conversion to rise to 71 from 46% (Table 1). It also affected M_V remarkably, it increased to 112 from 14 kDa. Conversion ratio was also controlled by monomer and xylan concentrations. Changing monomer concentration from 0.6 to 0.8 mol l^{-1} caused the conversion to increase to 75%, but M_V was determined very low (30 kDa). This occurrence was probably caused from rapidly reacting radical sites resulting in many small chains grafted on xylan. Xylan was the radical source of the reaction, so the amount of the xylan played a leading role on copolymerization. Reducing agent concentration had also a peak position for conversion at 0.5% (w/v) xylan giving 83% conversion and also the highest M_V obtained at these conditions for this part of the study (271 kDa). Higher xylan concentration (0.8%) yielded nearly no copolymer and probably resulted in oxidation.

As results showed, xylan and acrylonitrile concentrations were very important for high conversion ratios. Optimum condition was found as 5.36 mmol l^{-1} CAN in 0.2 mol l^{-1} perchloric acid gave maximum yield (83%) at 27 °C using 0.54% (w/v) xylan and 0.82 mol l^{-1} acrylonitrile for 1-h reaction; copolymer species obtained under these conditions were labeled as X–PAN$_{HClO_4}$.

3.2. *FTIR characterizations of polymers*

Characteristic vibration bands of xylan were at 3411 cm^{-1} O—H stretching, 2923 cm^{-1} C—H stretching, 1638 cm^{-1} H—O—H deformation of absorbed water as a broad band, 1200–920 cm^{-1} various C—O, C—C stretching, and C—O—H bendings (Kačuráková et al., 1999). Fig. 1 shows 1800–800 cm^{-1} region of FTIR spectra of the xylan, X–PAN copolymers, and PAN. Low intensity shoulder at 1159 cm^{-1} indicated the presence of arabinosyl side-chains, corresponding C—O—C vibrations in the anomeric region of the hemicellulose (Xiao et al., 2001). The band at 1088 cm^{-1} corresponded to the C—O—H bending, which was strongly influenced by degree of branching (Sun et al., 2000). The sharp band at 898 cm^{-1} was indicator of β-glycosidic linkages. Characteristic bands for PAN were determined as C—H stretching (2938 cm^{-1}), C≡N stretching (2244 cm^{-1}), C—H bending (1453 cm^{-1}) bands.

Spectra of X–PAN showed absorption bands at 2940 cm^{-1} (C—H stretchings), 3446 cm^{-1} (broad, O—H stretchings), 2244 cm^{-1} (sharp and intense, C≡N stretching), 1300–850 cm^{-1} (C—O, C—C stretchings, and C—O—C, C—O—H bendings).

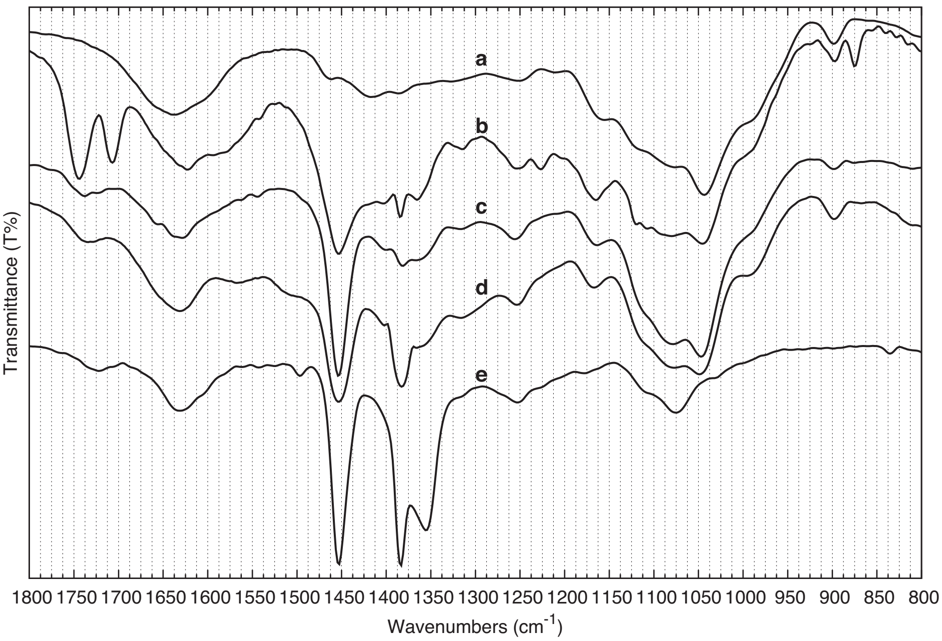

Fig. 1. Partial FTIR spectra of (a) xylan, (b) X–PAN$_{HClO_4}$ with 0.2% xylan, (c) X–PAN$_{HClO_4}$ with 0.5% xylan, (d) X–PAN$_{HNO_3}$, and (e) PAN homopolymer.

Certain absorption bands in spectra of X–PAN were assigned to C≡N (2244 cm) and anomeric group vibration signal of xylan (898 cm). As these bands are unique for acrylonitrile and xylan, they were compared to determine relative amount of grafting acrylonitrile onto xylan. Intensities of the absorption bands were adjusted with intensity of signal at 1453 cm^{-1}, which was base signal for all spectra. Then proportioning C≡N to anomeric signal gave ratio of acrylonitrile to xylan and results were given in Table 1. X–PAN$_{HNO_3}$ showed small value of the proportion (9.6) while X–PAN$_{HClO_4}$ had a higher value (16.7) although they had close M_V. These results showed that xylan degraded in HNO_3 under used conditions giving small portions of xylan chains, however, $HClO_4$ conditions did not cause degradation of xylan that much.

Also a remarkable change occurred for copolymers in 1100–1000 cm^{-1} region (Fig. 1b–d). The band at 1076 cm^{-1}, which was associated with the degree of branching, shifted to higher frequencies in the cases of copolymers. Explanation for this occurrence could be proposed as acrylonitrile grafted onto xylan conformation changed. Mentioned absorption band was strongly influenced from branching, in other words it was very closely related with the conformation of the main chain. Significant change of the pattern in this region also supported this occurrence. This relation was observed in experiments with different xylan/acrylonitrile ratio. As the ratio goes higher, xylan was used in higher amount, branching was smaller, so the band was observed as a shoulder to 1042 cm^{-1}. However, as acrylonitrile ratio increased, molecular weight of the grafted PAN would be higher forcing xylan to change the conformation of the main chain, and this caused the band at 1078 cm^{-1} to be strengthened.

Another important signal was observed about 1740–1700 cm^{-1} probably due to oxidation products of ceric ion–xylan reaction (Scheme 2). Xylan had no signal in this region (Fig. 1a), however, PAN had a weak signal at 1722 cm^{-1} probably due to oxidation of acrylonitrile during polymerization (Fig. 1e). Copolymers' FTIR spectra differed in this region with regard to the reaction conditions. X–PAN$_{HClO_4}$ (Fig. 1c) showed a band at 1738 cm^{-1} mainly for oxidation and linkage-related (anomeric) signal fairly shifted (ca. 0.3 cm^{-1}) to lower frequency. Although conversions were too close, X–PAN$_{HClO_4}$, which were synthesized using 0.2 and 0.5% xylan (conversions were 75 and 83%), spectra were different quietly like their M_V. Two major bands were observed at 1744 and 1707 cm^{-1} for copolymer synthesized using 0.2% xylan (Fig. 1b). There was also

Table 1
Summary table for 1-h polymerization reactions, stock CAN solutions were prepared with indicated catalyst.

Temp. (°C, ±1)	[catalyst] (mol l^{-1})	[CAN] (mmol l^{-1})	[AN] (mol l^{-1})	[Xylan] (%, w/v)	Conversion[a] (%)	M_V (kDa)	CN:X[b]
HNO_3							
70	0.5	18.1	0.5	0.2	57	102	22.7
50	0.5	18.1	0.5	0.2	77	139	24.3
35	0.5	18.1	0.5	0.2	22	8	10.5
50	0.1	18.1	0.5	0.2	64	62	9.3
50	0.1	21.7	0.5	0.2	96	249	9.6
50	0.5	18.1	0.5	0.5	76	242	10.6
$HClO_4$							
27	0.1	5.5	0.6	0.2	–	–	–
27	0.2	5.5	0.6	0.2	46	14	9.2
27	0.2	10.9	0.6	0.2	71	112	10.5
27	0.2	5.4	0.8	0.2	75	30	9.4
27	0.2	5.4	0.8	0.5	83	271	16.7
27	0.2	5.4	0.8	0.9	–	–	–

[a] $W/W_0 \times 100$, W = copolymer (g), W_0 = monomer (g)+ xylan (g).
[b] Intensity ratio of FTIR signals for CN (2244 cm^{-1}) and xylan (898 cm^{-1}) relative to signal at 1453 cm^{-1}.

Table 2
DSC data of PAN homopolymer and X–PAN copolymers.

Polymer	T_g (°C)	ΔC_p (mJ g^{-1} °C^{-1})	$T_{d,max}$ (°C)	ΔQ (J g^{-1})
Xylan	−30.6	43.5	285.8	132.6
PAN	–	–	312.6	254.6
X–PAN$_{HNO_3}$	−30.5	45.7	291.1	379.6
X–PAN$_{HClO_4}$	−30.0	24.5	296.5	422.1

an additional band at 875 cm^{-1} indicating that conformation of the main xylan chain changed greatly, as this region was related with anomeric connections. X–PAN$_{HNO_3}$ also showed very low oxidation relying on the signal at 1734 cm^{-1}, and it had also very small shift for anomeric band (ca. 0.4 cm^{-1}) indicating that conformation fairly changed.

Changes in the intensity and peak position of the bands implied that reaction conditions greatly affected properties of obtained product. Temperature caused this signal to increase while using HNO$_3$, probably causing oxidation path more favorable for xylan than polymerization. In the case of perchloric acid employed polymerization reactions, xylan concentration had a control over this signal. Lower xylan concentrations caused intensity of the signal to rise, however, increasing the concentration leads to a decrease in the intensity.

3.3. *Thermal characterizations of polymers*

Thermal analyses of homopolymer (PAN), copolymers (X–PAN$_{HNO_3}$ and X–PAN$_{HClO_4}$) and xylan were conducted using differential scanning calorimeter (DSC) and thermogravimetric analysis (TGA).

3.3.1. *Differential scanning calorimeter (DSC) measurements*

Characterizations were conducted manipulating DSC data of the samples which can be summarized as follows. Glass transition temperature (T_g) was identified as a break at baseline and was determined as a peak on first derivative of specific heat flow versus temperature plot. Change in specific heat capacity (ΔC_p) was determined as difference between levels of glass transition (Menczel, Judovits, & Prime, 2009). Temperature in which maximum decomposition ($T_{d,max}$) occurred was determined as a peak position in first derivative of specific heat flow versus temperature plot. Heat of decomposition (ΔQ) was obtained from integration of decomposition signal on plot of specific heat flow versus time.

Results of DSC analyses are summarized in Table 2 and DSC thermograms of PAN, X–PAN$_{HNO_3}$ and X–PAN$_{HClO_4}$ are plotted in Fig. 2. A weak endothermic shoulder appeared on xylan's thermogram about 175 °C due to softening (Ramiah, 1970), and then thermal degradation and decomposition took place above 200 °C. In this region first an endothermic signal appeared having a peak position 225.5 °C, then came strong exothermic signals having a peak position at 274.0 °C. These signals were caused from thermal degradation of xylan, indicating that decomposition reactions had different mechanisms. Maximum degradation took place at 285.8 °C for xylan, having a decomposition heat (ΔQ) 132.6 J g^{-1}. Thermal events for PAN summarized as an exothermic signal due to autocatalytic decomposition reaction (Dunn & Ennis, 1970) giving a peak at 312.6 °C with ΔQ of 254.6 J g^{-1}. In the case of copolymers thermal events showed PAN characteristics with regard to molecular weight. Molecular weight increase caused a shift in maximum degradation temperature to higher values, i.e. X–PAN$_{HClO_4}$ had a $T_{d,max}$ at 296.5 °C, and X–PAN$_{HNO_3}$ at 291.1 °C. Besides, ΔQ value was the highest for X–PAN$_{HClO_4}$ (422.1 J g^{-1}). This occurrence could be attributed to decomposition reaction, as xylan decomposed smaller chains of acrylonitrile polymer degraded faster giving higher amounts of energy. This conclusion also supported with higher ΔQ value of X–PAN$_{HNO_3}$ (379.6 J g^{-1}) than PAN.

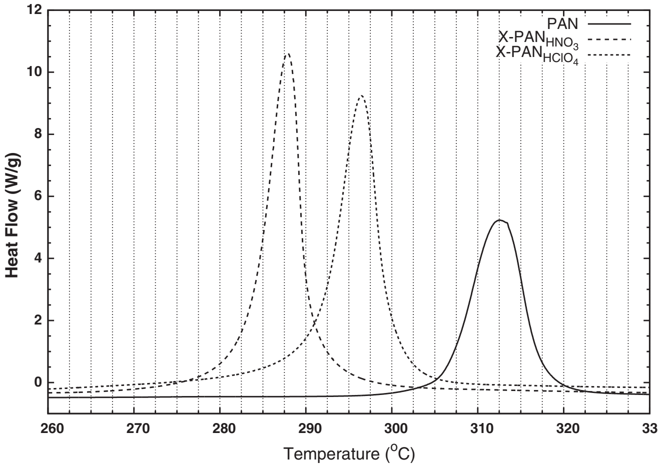

Fig. 2. DSC thermograms of PAN and X–PAN copolymers which were obtained at optimum conditions.

Xylan showed a T_g at −30.6 °C, but PAN showed no T_g in measurement range. Copolymers showed slightly different T_g values, X–PAN$_{HNO_3}$ −30.5 °C, X–PAN$_{HClO_4}$ −30.0 °C. These small differences could be attributed to changes in conformation and oxidation of xylan during polymerization. Decrease in specific heat capacity also supported this occurrence. Xylan and X–PAN$_{HNO_3}$ showed slightly different values, 43.5 and 45.7 mJ g^{-1} °C^{-1}, while X–PAN$_{HClO_4}$ had a value of 24.5 mJ g^{-1} °C^{-1}. This decrease could be related with both polymerization and side reactions such as oxidation and degradation of xylan. The smaller value of ΔC_p for X–PAN$_{HClO_4}$ could be attributed to higher oxidation potential of HClO$_4$, as it probably oxidized xylan more than HNO$_3$ leading to a decrease of amorphous sites of final product.

In conclusion thermal properties were strongly affected from xylan content of copolymer. Xylan had a decomposition temperature at 285.8 °C, while PAN had 312.6 °C. Copolymers showed decomposition maxima between these two values.

3.3.2. *Thermogravimetric analysis (TGA) measurements*

Maximum decomposition temperature (T_{max}) was identified using first order derivative of weight loss versus temperature plot, T_{25} was temperature in which 25% loss occurred and W_{300} was residue at 300 °C. TGA data were evaluated in order to calculate activation energy of decomposition following literature cited (Broido, 1969). Activation energy was obtained from the plot of equation;

$$\ln \ln \left(\frac{1}{y}\right) = \left(\frac{E_a}{R}\right) \frac{1}{T} \qquad (1)$$

where E_a was activation energy in kJ mol^{-1}, R was gas constant in J mol^{-1} K^{-1}, T was temperature in K, and y was the fraction which was defined as

$$y = \frac{W_t - W_\infty}{W_0 - W_\infty} \qquad (2)$$

where W_t, W_∞, and W_0 were weights at temperature t, end of decomposition, and beginning of decomposition. Inverse absolute temperature was plotted against ln ln(1/y), then linear regression was applied and E_a was calculated from the slope of the linear function. TGA analyses of the samples are summarized in Table 3.

TGA thermograms of xylan, PAN, X–PAN$_{HNO_3}$ and X–PAN$_{HClO_4}$ are plotted in Fig. 3. Maximum decomposition temperatures were quite consistent with DSC data. Xylan and PAN showed maximum decomposition at 282.5 and 316.6 °C, supporting DSC where they showed similar values. Weight loss of 25% was observed at

Table 3
TGA data of xylan, PAN homopolymer and X–PAN copolymers.

Sample	T_{max}[a] (°C)	T_{25}[b] (°C)	W_{300}[c] (%, w/w)
Xylan	282.5	249.8	38.3
PAN	316.6	324.0	96.5
X–PAN$_{HNO_3}$	290.6	300.1	75.1
X–PAN$_{HClO_4}$	301.0	308.2	86.4

[a] Maximum degradation temperature.
[b] Temperature which 25% weight loss occurred.
[c] Residue at 300 °C.

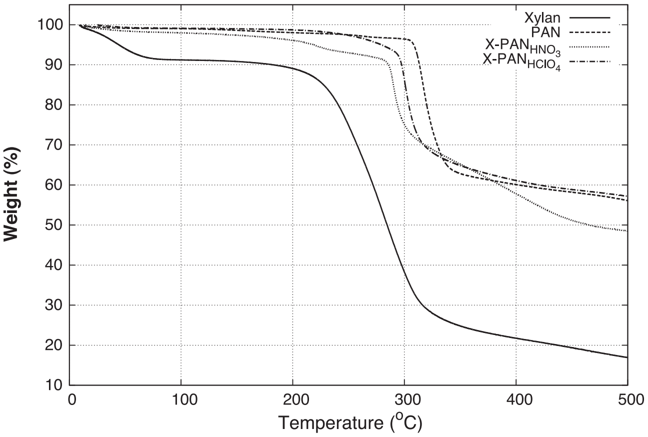

Fig. 3. TGA thermograms of xylan, PAN and X–PAN copolymers which were obtained at optimum conditions.

324.0 °C for PAN and 249.8 °C for xylan, but 9.1% loss of xylan occurred before 100 °C indicating water loss. Copolymers showed values between these limits (300.1 °C for X–PAN$_{HNO_3}$ and 308.2 °C for X–PAN$_{HClO_4}$, again. But a little water adsorption was observed for X–PAN$_{HNO_3}$ relying upon the loss before 100 °C (≈1%), unlike X–PAN$_{HClO_4}$, which adsorbed nearly no water. Xylan kept 38.3% of its initial weight at 300 °C, where this value was 96.5 for PAN, 75.1 for X–PAN$_{HNO_3}$, and 86.4 for X–PAN$_{HClO_4}$. All of these data indicated that grafted acrylonitrile onto xylan had lower thermal stability than PAN homopolymer, as expected.

Activation energy of decomposition (E_a) was calculated from slope with the highest correlation coefficient. Working range was determined as maximum weight loss region for all samples (200–400 °C). Decomposition range was divided into five sections which are stated in Table 4. First region was only observed for xylan between 200 and 250 °C having a value of 103.7 kJ mol^{-1}. Between 250 and 300 °C second degradation step of xylan occurred with a lower activation energy (83.3 kJ mol^{-1}). Xylan's thermal behavior and E_a values were consistent with literature (121.6 and 86.9 kJ mol^{-1} (Ramiah, 1970)). PAN thermal degradation was estimated through four sections indicating four different types of degradation mechanisms. Degradation reactions took place between 250–280, 280–300, 300–350, and 350–380 °C and corresponding E_a values were estimated as 88.5, 34.8, 439.8, and 57.1. Like maximum decomposition temperature, activation energies of copolymers were found smaller than PAN. First decomposition of copolymers was detected between 250 and 280 °C as 37.2 and 84.4 kJ mol^{-1} for X–PAN$_{HNO_3}$ and X–PAN$_{HClO_4}$, respectively. Second step was detected as main decomposition step between 280 and 300 °C as 329.2 and 279.7 kJ mol^{-1}. Then X–PAN$_{HNO_3}$ showed 2 steps between 300 and 380 °C while X–PAN$_{HClO_4}$ showed only one. Lower E_a values indicated that degradation was realized easier than PAN homopolymer, as concluded with DSC results. Activation energy of decomposition values of copolymers was mainly affected from M_V.

Table 4
Results of activation energy calculations using TGA data.

Sample	M_V	E_a (kJ mol^{-1})				
		I	II	III	IV	V[a]
Xylan	45	103.7	83.3		–	–
PAN	1000	–	88.5	34.8	439.8	57.1
X–PAN	249	–	37.2	329.2	41.2	47.5
X–PAN	271	–	84.4	279.7	41.8	

[a] I = 200–250 °C; II = 250–280 °C; III = 280–300 °C; IV = 300–350 °C; V = 350–380 °C.

TGA results had a great consistency with DSC results, and thermal degradation took place at lower temperatures as molecular weight was lower. In addition copolymers need less energy for degradation than xylan and PAN homopolymer.

4. Conclusion

In this work two catalysts (nitric acid and perchloric acid) were used to see their effect on ceric ion initiated polymerization. Reaction temperature, time, catalyst type and concentrations for stock ceric salt solution, monomer concentration, reducing agent were changed to find optimum condition to obtain the maximum conversion. Results showed that desired copolymer could be obtained by adjusting reaction conditions.

Catalyst type caused change the reaction conditions; high conversion was obtained at 50 °C with nitric acid and at ambient temperature with perchloric acid. Molecular weight values of the copolymers were varied with regard to conditions; at optimum condition perchloric acid caused higher M_V than nitric acid. Thermal properties were strongly affected from M_V of copolymer.

Acknowledgement

This study is supported by Research Fund of Istanbul Technical University, Turkey (Project No: 32044).

References

Atici, O. G., Akar, A., Ayar, Y., & Mecit, O. (1999). Synthesis of block copolymers via redox polymerization. *Journal of Applied Polymer Science*, *71*, 1385–1395.

Broido, A. (1969). A simple, sensitive graphical method of treating thermogravimetric analysis data. *Journal of Polymer Science Part A-2: Polymer Physics*, *7*, 1761–1773.

Czappa, D. J., (1974). *The role of acid in the cerium (IV) oxidation of carbohydrates*. PhD. The Institute of Paper Chemistry.

Doner, L. W., & Hicks, K. B. (1997). Isolation of hemicellulose from corn fiber by alkaline hydrogen peroxide extraction. *Cereal Chemistry*, *74*, 176–181.

Dunn, P., & Ennis, B. (1970). Thermal analysis of polyacrylonitrile. Part I. The melting of polyacrylonitrile. *Journal of Applied Polymer Science*, *14*, 1795–1798.

Ebringerová, A., Hromádková, Z., Alföldi, J., & Hribalová, V. (1998). The immunologically active xylan from ultrasound-treated corn cobs: Extractability, structure and properties. *Carbohydrate Polymers*, *37*, 231–239.

Galioğlu, O., Soydan, A. B., Akar, A., & Saraç, A. S. (1994). Block/graft copolymer synthesis via ceric salt. *Die Angewandte Makromolekulare Chemie*, *214*, 19–28.

Gáspár, M., Juhász, T., Szengyel, Z., & Réczey, K. (2005). Fractionation and utilisation of corn fibre carbohydrates. *Process Biochemistry*, *40*, 1183–1188.

Kačuráková, M., Wellner, N., Ebringerová, A., Hromádková, Z., Wilson, R. H., & Belton, P. S. (1999). Characterisation of xylan-type polysaccharides and associated cell wall components by FT-IR and FT-Raman spectroscopies. *Food Hydrocolloids*, *13*, 35–41.

Khullar, R. (2008). Grafting of acrylonitrile onto cellulosic material derived from bamboo (*Dendrocalamus strictus*). *eXPRESS Polymer Letters*, *2*, 12–18.

Lutfor, M. R., Sidik, S., Haron, J., Rahman, M. Z. A., & Ahmad, M. (2003). Modification of sago starch by graft copolymerization. Effect of reaction conditions on grafting parameters. *International Journal of Polymeric Materials*, *52*, 189–201.

Menczel, J. D., Judovits, L., & Prime, R. B. (2009). Differential scanning calorimetry. In J. D. Menczel, & R. B. Prime (Eds.), *Thermal analysis of polymers, fundamentals and applications*. New Jersey: Wiley.

Mino, G., & Kaizerman, S. (1958). A new method for the preparation of graft copolymers. polymerization initiated by ceric ion redox systems. *Journal of Polymer Science*, *31*, 242–243.

Mishra, A., Clark, J. H., Vij, A., & Daswal, S. (2008). Synthesis of graft copolymers of xyloglucan and acrylonitrile. *Polymers for Advanced Technologies*, *19*, 99–104.

Nagarajan, S., & Srinivasan, K. S. V. (1998). Efficiency of ceric ions for oxidation and polymerization – A review. *Polymer Reviews*, *38*, 53–76.

Pamies, R., Cifre, J. H., del Carmen López Martínez, M., & de la Torre, J. G. (2008). Determination of intrinsic viscosities of macromolecules and nanoparticles. Comparison of single-point and dilution procedures. *Colloid & Polymer Science*, *286*, 1223–1231.

Pottenger, C. R., & Johnson, D. C. (1970). Mechanism of cerium (IV) oxidation of glucose and cellulose. *Journal of Polymer Science Part A-1: Polymer Chemistry*, *8*, 301–318.

Pourjavadi, A., & Zohuriaan-Mehr, M. J. (2002a). Modification of carbohydrate polymers via grafting in air. 1. Ceric-induced synthesis of starch-g-polyacrylonitrile in presence and absence of oxygen. *Starch – Stärke*, *54*, 140–147.

Pourjavadi, A., & Zohuriaan-Mehr, M. J. (2002b). Modification of carbohydrate polymers via grafting in air. 2. Ceric-initiated graft copolymerization of acrylonitrile onto natural and modified polysaccharides. *Starch – Stärke*, *54*, 482–488.

Ramiah, M. V. (1970). Thermogravimetric and differential thermal analysis of cellulose, hemicellulose, and lignin. *Journal of Applied Polymer Science*, *14*, 1323–1337.

Shibukawa, T., Sone, M., Uchida, A., & Iwahori, K. (1968). Light-scattering study of polyacrylonitrile solution. *Journal of Polymer Science Part A-1: Polymer Chemistry*, *6*, 147–159.

Solomon, O. F., & Ciuťa, I. Z. (1962). Détermination de la viscosité intrinsèque de solutions de polymères par une simple détermination de la viscosité. *Journal of Applied Polymer Science*, *6*, 683–686.

Sun, R., Tomkinson, J., Geng, Z. C., & Wang, N. J. (2000). Comparative studies of hemicelluloses solubilized during the treatments of maize stems with peroxymonosulfuric acid, peroxyformic acid, peracetic acid, and hydrogen peroxide. Part 1. Yield and chemical characterization. *Holzforschung*, *54*, 349–356.

Ünlü, C. H., Günister, E., & Atıcı, O. (2009). Synthesis and characterization of NaMt biocomposites with corn cob xylan in aqueous media. *Carbohydrate Polymers*, *76*, 585–592.

Xiao, B., Sun, X. F., & Sun, R. (2001). Chemical, structural, and thermal characterizations of alkali-soluble lignins and hemicelluloses, and cellulose from maize stems, rye straw, and rice straw. *Polymer Degradation and Stability*, *74*, 307–319.